EUKARYOTIC CELL, June 2007, p. 960–970 Vol. 6, No. 6
1535-9778/07/$08.00+0 doi:10.1128/EC.00047-07

Further Characterization of the Signaling Proteolysis Step in the *Aspergillus nidulans* pH Signal Transduction Pathway▽‡

María M. Peñas,[1]† América Hervás-Aguilar,[2] Tatiana Múnera-Huertas,[1] Elena Reoyo,[2] Miguel Á. Peñalva,[2] Herbert N. Arst, Jr.,[1] and Joan Tilburn[1]*

Department of Molecular Microbiology and Infection, Imperial College London, The Flowers Building, London SW7 2AZ, United Kingdom,[1] and Departamento de Microbiología Molecular, Centro de Investigaciones Biológicas, CSIC, Ramiro de Maeztu, 9, Madrid 28040, Spain[2]

Received 16 February 2007/Accepted 28 March 2007

The *Aspergillus nidulans* pH-responsive transcription factor PacC is modulated by limited, two-step proteolysis. The first, pH-regulated cleavage occurs in the 24-residue highly conserved "signaling protease box" in response to the alkaline pH signal. This is transduced by the Pal signaling pathway, containing the predicted calpain-like cysteine protease and likely signaling protease, PalB. In this work, we carried out classical mutational analysis of the putative signaling protease PalB, and we describe 9 missense and 18 truncating loss-of-function (including null) mutations. Mutations in the region of and affecting directly the predicted catalytic cysteine strongly support the deduction that PalB is a cysteine protease. Truncating and missense mutations affecting the C terminus highlight the importance of this region. Analysis of three-hemagglutinin-tagged PalB in Western blots demonstrates that PalB levels are independent of pH and Pal signal transduction. We have followed the processing of MYC_3-tagged PacC in Western blots. We show unequivocally that PalB is essential for signaling proteolysis and is definitely not the processing protease. In addition, we have replaced 15 residues of the signaling protease box of MYC_3-tagged PacC (*pacC900*) with alanine. The majority of these substitutions are silent. Leu481Ala, Tyr493Ala, and Gln499Ala result in delayed PacC processing in response to shifting from acidic to alkaline medium, as determined by Western blot analysis. Leu498Ala reduces function much more markedly, as determined by plate tests and processing recalcitrance. Excepting Leu498, this demonstrates that PacC signaling proteolysis is largely independent of sequence in the cleavage region.

The activities of an increasing number of proteins, including a number of transcription factors, have been shown to be modulated by limited and site-specific proteolysis. One important mechanism involving incomplete proteasomal degradation, known as regulated ubiquitin proteasome-dependent processing (RUP) (31), mediates the proteolytic activation of transcription factors NF-κB1, NF-κB2, and the yeast NF-κB-like proteins Spt23p and Mga2p (5, 23, 49; reviewed in references 55 and 56). Other RUP substrates include *Drosophila* Cubitus interruptus (Ci) and one of its vertebrate homologs, glioma-associated protein (Gli3), which in the absence of Hedgehog (Hh) signaling are converted from the Ci155 and Gli3-190 activators of Hh target genes to the Ci75 and Gli3-83 respective repressors of Hh target genes (3, 10, 50, 54, 67). Regulated intramembrane proteolysis (RIP) is a process whereby certain proteins are released from a membrane-bound sequestered state by a process essentially involving an intramembrane cleaving protease. The intramembrane cleaving protease cleavage usually proceeds constitutively, following a regulated primary extramembrane cleavage which tailors its substrate (reviewed in references 7, 40, 72, and 76). Other modulatory proteolytic processes involve cysteine proteases acting independently of RUP and RIP and potentially numerous instances involving members of the calpain superfamily (28, 70, 74; reviewed in references 9, 27, 62, and 66). They also include the alkaline ambient pH-triggered proteolytic modulation of the *Aspergillus nidulans* PacC pH-regulatory transcription factor, which shares features of its DNA binding domain with Gli family transcription factors (22). PacC processing resembles both RUP and RIP in certain respects and involves a calpain-like protein, as in the *Saccharomyces cerevisiae* single-step proteolytic activation of the PacC ortholog Rim101p.

In the current model (Fig. 1), under acidic growth conditions, the full-length form of PacC, $PacC^{72}$, predominantly assumes a processing protease-inaccessible "closed conformation" which is maintained by interactions involving three regions, including the negatively acting C terminus (21). Under alkaline conditions, $PacC^{72}$ undergoes a two-step proteolysis (17, 42, 48) to form $PacC^{27}$, an activator of alkaline-expressed genes (20) and a repressor of acid-expressed genes (17, 19, 20, 42, 48). The first of the two steps, as in RIP, is the regulated, in this case alkaline ambient pH-dependent, step. This results in the formation of $PacC^{53}$ from $PacC^{72}$, the signaling proteolysis step, which corresponds to the single cleavage which occurs in *S. cerevisiae* in response to alkaline pH (37, 38; reviewed in references 2, 52, and 53).

In *A. nidulans*, signaling proteolysis occurs in response to the functioning of the six-membered Pal signal transduction pathway (1). PalH, which has two homologs in *S. cerevisiae*, Rim21p

* Corresponding author. Mailing address: Department of Molecular Microbiology and Infection, Imperial College London, The Flowers Building, Armstrong Road, London SW7 2AZ, United Kingdom. Phone: 44 207 594 3187. Fax: 44 207 594 3095. E-mail: j.tilburn@imperial.ac.uk.

† Present address: Departamento de Producción Agraria, Universidad Pública de Navarra, Campus de Arrosadia s/n, Pamplona (Navarra) 31006, Spain.

‡ Supplemental material for this article may be found at http://ec.asm.org/.

▽ Published ahead of print on 6 April 2007.

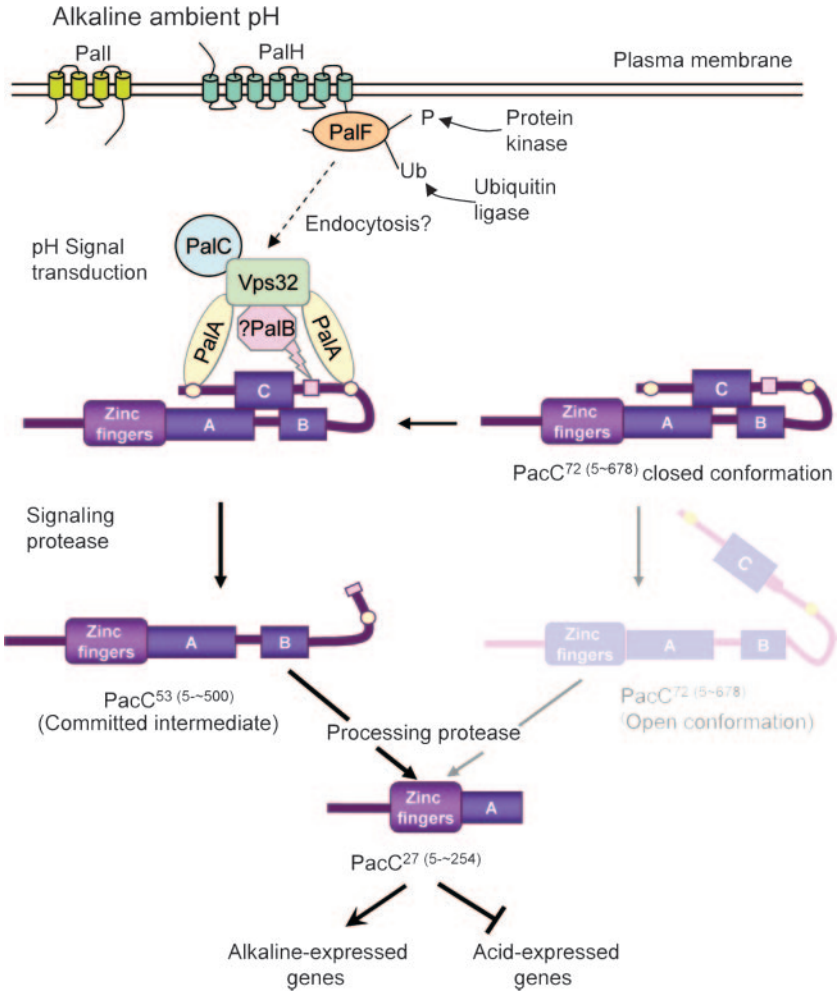

FIG. 1. Model of PacC two-step processing. Codon 5 is the physiological *pacC* initiation codon (42). It is not known if PalA and PalC interact with Vps32 simultaneously or sequentially.

and Dfg16p, and PalI (*S. cerevisiae* Rim9p) are predicted seven- and four-transmembrane domain proteins (4, 38, 46). PalF (*S. cerevisiae* Rim8p) (38, 39), an arrestin-related protein, strongly binds the cytoplasmic tail of PalH and is phosphorylated and ubiquitinated in a fashion dependent on alkaline pH, PalH, and partially PalI (15, 30, 38). It has been proposed that PalF phosphorylation and ubiquitination lead to the endocytosis of the PalF-PalH complex, transducing the pH signal to the downstream components (30). PalA (*S. cerevisiae* Rim20p) (45, 78) contains a BRO1 domain (36, 47) which interacts with Vps32 protein family members (34, 35, 51, 64, 73, 75, 78, 79). PalA is thought to connect $PacC^{72}$ with Vps32 of the endosomal sorting complex required for transport III (73). PalC (46), like PalA, contains a BRO1 domain (68) through which it also interacts with Vps32 (A. Galindo, A. Hervás-Aguilar, O. Rodriguez-Galán, O. Vincent, H. N. Arst, Jr., J. Tilburn, and M. Á. Peñalva, submitted for publication).

PalB (*S. cerevisiae* Rim13p) is the likely signaling protease (16, 37, 63). PalB and Rim13p (also known as Cpl1p) resemble the large subunits of *m*- or μ-calpain, which are modulatory proteases which recognize bonds between domains rather than specific sequences and hydrolyze proteins in a limited manner (reviewed in reference 66). PalB and Rim13p contain the characteristic Cys, His, and Asn active-site residues but lack the calmodulin-like calcium binding domain IV (16, 27). By analogy with *S. cerevisiae*, where Rim13p has been shown to interact with Vps32p, it has been suggested that signaling proteolysis involves a complex of Vps32, PalA, PalB, and PacC on endosomal membranes, in agreement with the model described for *S. cerevisiae* (29, 33, 78, 79; reviewed in references 2 and 53).

Signaling proteolysis occurs between PacC residues 493 and 500 within a highly conserved 24-residue signaling protease box. Deletion of the box or substitution of Leu498 within the box by serine prevents signaling proteolysis (17). The resulting transient processing intermediate, $PacC^{53}$, has an open conformation (17) and is accessible to the processing protease, which removes approximately 250 C-terminal residues (42, 48). This occurs in a pH-independent manner and to a point which is determined by sequences or structures remote from and amino-terminal to it (42, 48). This resembles RUP in NF-κB p100 and p105 and Ci, where a tightly folded domain preceded by a low-complexity sequence in the path of the proteasome prevents total degradation (5, 67). Trace amounts of $PacC^{27}$

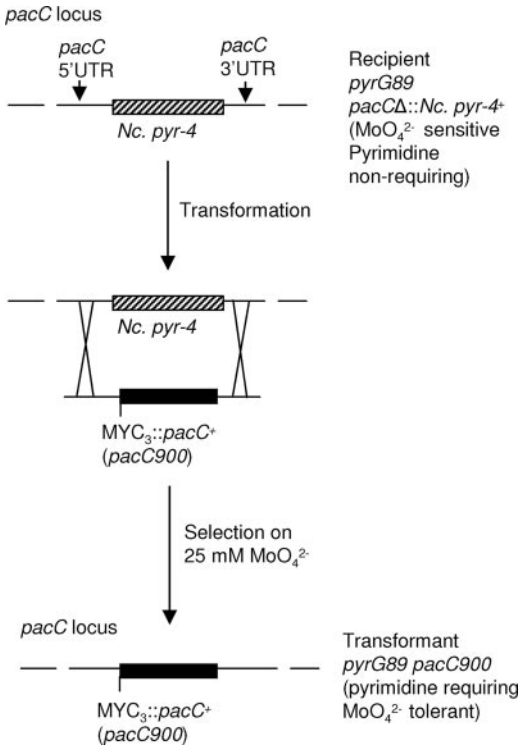

FIG. 2. MYC_3-tagging *pacC* by gene replacement. *Nc.*, *Neurospora crassa*.

detected in the absence of signaling proteolysis have been attributed to the processing of a very minor proportion of PacC[72] which has assumed an "open conformation," allowing access to the processing protease without the removal of the C terminus (Fig. 1) (15–17, 19, 21, 42, 46, 48; reviewed in reference 53).

The approximate site of the signaling proteolysis has been determined, and PalB is the obvious (and currently sole) candidate for the signaling protease (17). However, neither the precise identity of the signaling protease nor its specificity requirements have been determined definitively. In this work we further characterize the features of the candidate signaling protease and the sequence requirements in the cleavage region of its substrate.

MATERIALS AND METHODS

***A. nidulans* growth and phenotype testing.** *A. nidulans* gene symbols and classical genetic techniques follow the work of Clutterbuck (12). Phenotype testing of *pacC* mutations by growth tests and colony staining has been described in the work of Tilburn et al. (69) and references therein. Mycelia for protein extraction were grown at 37°C with shaking at 200 to 250 rpm. pH-shifted mycelia were grown for 16 h in acidic MFA medium and transferred to alkaline MFA medium for the times indicated in Fig. 4, 5, and 8. MFA medium is minimal medium minus glucose (13) containing 2.5% (wt/vol) corn steep liquor (Sigma) and 3% sucrose. Acidic medium was buffered with 50 mM citrate, giving an initial pH value of ~4.3. Alkaline medium was buffered with 100 mM HEPES, pH ~8.3, at the time of transfer. Mycelia grown under steady-state conditions were incubated for 16 h in acidic or alkaline MFA buffered with 100 mM NaH_2PO_4 plus 100 mM NaCl (pH ~5) and 100 mM Na_2HPO_4 (pH ~8), respectively.

Selection of *palB* mutations characterized in this work. *palB111* was selected after *N*-methyl-*N*′-nitro-*N*-nitrosoguanidine mutagenesis as enabling growth of the *biA1 areA*^{r}*2 fwA1* strain on 5 mM γ-aminobutyrate (GABA) as the sole nitrogen source. *palB16*, *-37*, *-38*, and *-39* were obtained in the same reversion experiment as that described by Arst et al. (1) for *palH17* and *palI30*. *palB70* was a kind gift from Eduardo A. Espeso (unpublished data). *palB500 to -524* were selected after UV mutagenesis as enabling utilization of 5 mM GABA as the nitrogen source in diploid, *pabaA1 areA*^{r}*5 glrA1 argC3 tubA1 palB7 chaA1 pantoA10*/*areA*^{r}*5 inoB2*, and following benlate haploidization and subsequent purification, *argC*$^+$ *tubA*$^+$ *chaA*$^+$ *pantoA*$^+$ haploids were obtained carrying the new *palB*$^-$ mutations. This diploid represents an optimization of the *pal*$^-$ diploid selection technique described in reference 68, since it allows selection in haploidization against markers closely linked to *palB*7 on the centromere-proximal side (*argC3* and *tubA1*, resulting in arginine requirement and hypersensitivity to benlate, respectively) and contains two centromere-distal markers (*chaA1* and *pantoA10*), which allow selection against and detection of mitotic recombination. (*argC* is actually on chromosome VII, but *argC3* is a VII-VIII translocation.) *palB7* and *palB11* (originally designated *palE11* but subsequently shown to be allelic to *palB7* [1]) were selected by Dorn (18).

TABLE 1. MYC_3-tagged *pacC* alleles and strains constructed and characterized in this work[a]

Allele	Change(s) in protein	Nucleotide change(s)	Strain name	Genotype	Result by Western analysis
pacC900(*L481A*)	L481A	C2399G T2400C	MP87	*pacC900*(*L481A*)	+
pacC900(*G482A*)	G482A	G2403C	MP123	*pacC900*(*G482A*)	−
pacC900(*F485A*)	F485A	T2411G T2412C	MP91	*yA2 pacC900*(*F485A*)	+
pacC900(*D486A*)	D486A	A2415C	MP114	*yA2 pabaA1 pacC900*(*D486A*)	+
pacC900(*D488A*)	D488A	A2421C	MP84	*yA2 inoB2 pacC900*(*D488A*)	+
pacC900(*E489A*)	E489A	A2424C	MP160	*yA2 pabaA1 inoB2 pacC900*(*E489A*)	+
pacC900(*R490A*)	R490A	C2426G G2427C	MP82	*pacC900*(*R490A*)	−
pacC900(*R491A*)	R491A	C2429G G2430C	MP79	*pacC900*(*R491A*)	+
pacC900(*R491A Q499A*)	R491A	C2429G G2430C	MP116	*inoB2 pacC900*(*R491A Q499A*)	+
	Q499A	C2453G A2454C			
pacC900(*R492A*)	R492A	A2432G G2433C	MP121	*yA2 pabaA1 pacC900*(*R492A*)	−
pacC900(*Y493A*)	Y493A	T2435G A2436C	MP104	*inoB2 pacC900*(*Y493A*)	+
pacC900(*T494A*)	T494A	A2438G	MP94	*yA2 pabaA1 pacC900*(*T494A*)	+
pacC900(*G495A*)	G495A	G2442C	MP100	*pacC900*(*G495A*)	+
pacC900(*G496A*)	G496A	G2445C	MP98	*pacC900*(*G496A*)	−
pacC900(*L498A*)	L498A	T2450G	MP190	*adE20 pyroA4 pacC900*(*L498A*)	+
pacC900(*L498F*)	L498F	G2452C	MP212	*adE20 pacC900*(*L498F*)	+
pacC900(*L498S*)	L498S	T2451C	MP176	*adE20 pacC900*(*L498S*)	+
pacC900(*Q499A*)	Q499A	C2453G A2454C	MP76	*inoB2 pacC900*(*Q499A*)	+
pacC900	None	None		*yA2 pabaA1 pacC900*	+

[a] Amino acids and nucleotides are as described by Tilburn et al. (69).

TABLE 2. *palB* mutations characterized in this work[a]

Allele	Nucleotide change	Change in protein	Growth at pH 8.0[d]		Mutagen method	Selection	Reference
			20°C	37°C			
Wild type	None	None	+++++	+++++	None	None	8, 67
Truncating mutations							
palB508	T340G	L13stop	−	−	UV	Diploid GABA	This work
palB510	T340A	L13stop	−	−	UV	Diploid GABA	This work
palB70	A359T	PSD	ND	−	None	Haploid GABA	E. A. Espeso (unpublished)
palB38	A515T	K55stop	−	−	UV	Haploid GABA	This work
palB509	del(658-662)	R103fs[c]	−	−	UV	Diploid GABA	This work
palB502	T678G	L109stop	−	−	UV	Diploid GABA	This work
palB501	C680T	Q110stop	−	−	UV	Diploid GABA	This work
palB518	T849C	PSD	++	+/−	UV	Diploid GABA	This work
palB520	A866T	K144stop	−	−	UV	Diploid GABA	This work
palB519	A1638T	K385stop	−	−	UV	Diploid GABA	This work
palB500	G1767T	E428stop	−	−	UV	Diploid GABA	This work
palB505	delA2007	K508fs	−	−	UV	Diploid GABA	This work
palB513	T2140G	L552stop	−	−	UV	Diploid GABA	This work
palB511	delG2801 A2803G	Y773fs	−	−	UV	Diploid GABA	This work
palB111	G2784T	E767stop	−	−	NTG	Haploid GABA	This work
palB7	G2856T	G791stop	+/−	−	UV	Lack of alkaline phosphatase	18
palB11[b]	del(G2863-C2873)	R793fs	−	−	UV	Lack of alkaline phosphatase	18
palB37	G2925T	E814stop	+/−	−	UV	Haploid GABA	This work
Missense mutations							
palB517	T1027G G1029T	D197E C198F	−	−	UV	Diploid GABA	This work
palB16	GT(1034 1035)AA	V200N	−	−	UV	Haploid GABA	This work
palB504	T1405G	L307R	+	−	UV	Diploid GABA	This work
palB524	T2388A	I618L	++++	+++	UV	Diploid GABA	This work
palB39	T2340C	S619P	+++	−	UV	Haploid GABA	This work
palB515	T2713C	L743P	++	−	UV	Diploid GABA	This work
palB516	A2778C T2783C	T765P	++	−	UV	Diploid GABA	This work
palB503	T2875C	F797S	+++	+++	UV	Diploid GABA	This work
palB514	T2923C	L813P	++	−	UV	Diploid GABA	This work

[a] Nucleotides and amino acids are numbered as in GenBank Z54244. PSD, predicted splicing defect; ND, not determined; NTG, *N*-methyl-*N*′-nitro-*N*-nitrosoguanidine.

[b] Formerly *palE11*; see the work of Arst et al. (1). The *palB11* phenotype, which is more extreme than that of the more N-terminal nonsense *palB7* mutation, is possibly influenced by 17 out-of-frame residues at the C terminus of the protein.

[c] fs, frameshift.

[d] −, no growth; +/−, very small amount of growth; + to +++++, increasing amounts of growth from small to wild-type.

MYC_3 tagging of PacC. A triplicated MYC epitope coding sequence, i.e., MLA EQKLISEEDLNG EQKLISEEDLNG EQKLISEEDLNG (44), was amplified from plasmid pMPY-3xMYC (60) with attachment of terminal NcoI targets. This fragment was subcloned into the NcoI site overlapping the major PacC initiation codon in pSpacC (17) to give pSpacC900, which was used to introduce the MYC_3-tagged wild-type *pacC* allele, designated *pacC900*, into the *pacC* resident locus. Gene replacements were carried out using a strain carrying the *pyrG89* mutation (resulting in pyrimidine auxotrophy) at the resident locus and with the orthologous *Neurospora crassa pyr-4* gene replacing the entire *pacC* coding region (69). Transformation was carried out using linearized fragments containing the *pacC* moiety of the plasmid, as shown in Fig. 2. Transformants moderately tolerant of 25 mM sodium molybdate were selected following transformation (69). These transformants were then tested for loss of *pyr-4* (i.e., for pyrimidine auxotrophy) resulting from the expected gene replacement, which was confirmed by Southern blot analyses. *pyrG89* and other undesired markers were then removed from selected strains by sexual crossing with a (*pyrG*$^+$) *glrA*1 strain (*glrA* is closely linked to *pacC*, such that *glrA*$^+$ strains have a 98% chance of carrying *pacC900*). The presence of the *pacC900* allele was confirmed with a *glrA*$^+$ strain.

New MYC_3-tagged *pacC* alleles. The MYC_3-tagged *pacC* mutant alleles created and characterized in this work are described in Table 1. These site-directed mutations with alanine residues replacing different amino acid residues within the conserved signaling proteolysis box (17) were obtained using a Stratagene QuikChange site-directed mutagenesis kit according to the manufacturer's recommendations using plasmid pSpacC900 (see above) as a template and the mutagenic primers described in Table S1 in the supplemental material. The pSpacC900$^{R491A\ Q499A}$ plasmid was obtained serendipitously, probably by contamination of the R491 mutagenic reaction with one of the Q499 primers (see Table S1 in the supplemental material). The mutated *pacC* moieties of the constructs were transformed as linear fragments into a *pacC* deletion strain as described for *pacC900* (Results and Discussion) (Fig. 2) except that molybdate was used at 12.5 mM in the selection plates (17). The presence of desired mutations and the absence of additional mutations were confirmed by sequencing PCR products containing the entire *pacC* coding region obtained from transformant DNA.

Three-hemagglutinin (HA_3)-tagged PalB. A strain carrying a *palB*::HA_3 allele (E. Díez and M. Á. Peñalva, unpublished) was crossed with *palF15*, *palC4*, *palA1*, *palH17*, and *palI32* strains to obtain double mutants, and all strains were used to determine the effects of pH and pH signal transduction on PalB levels.

Western blot analysis. Mycelia were harvested on Miracloth, pressed dry, frozen in small 200- to 300-mg amounts in liquid nitrogen, and lyophilized overnight. Proteins were extracted as described previously (24). Protein samples were precipitated with 10% trichloroacetic acid, washed with ethanol:ether (1:1 and then 1:3), and resuspended in loading buffer (62.5 mM Tris [pH 8.3], 2% sodium dodecyl sulfate, 5% β-mercaptoethanol, 6 M urea, 0.05% bromophenol blue) and denatured by heating to 100°C for 5 min. Fifty-microgram protein samples were resolved on 0.1% sodium dodecyl sulfate–10% acrylamide gels before electrotransfer to a nitrocellulose membrane. For detection of MYC_3::PacC, the membranes were incubated with anti-c-MYC mouse monoclonal antibody (9E10; Santa Cruz Biotechnology) at a 1/1,000 dilution and usually overnight at

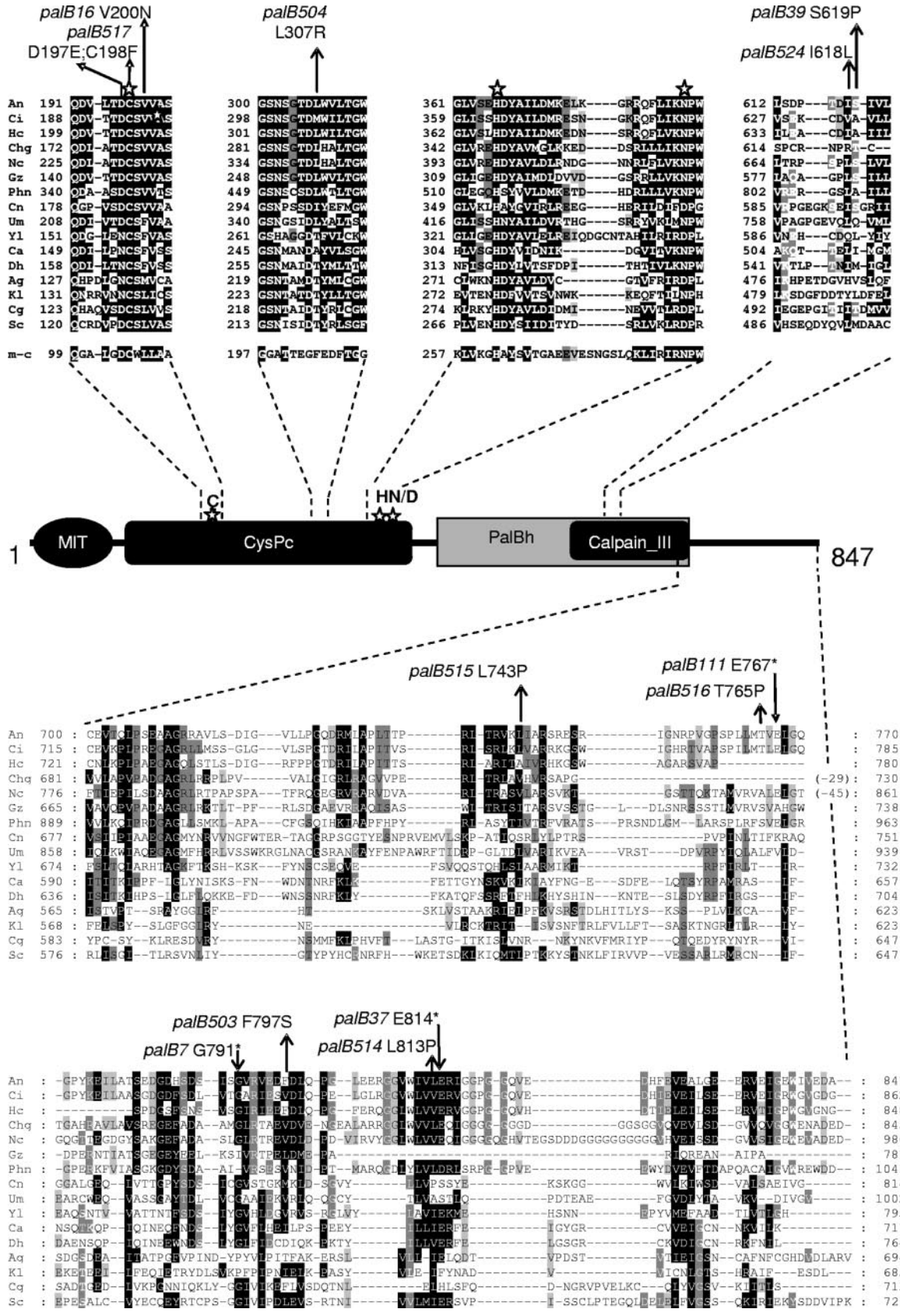

FIG. 3. Sequence features of PalB and *palB* mutations. Recognized domains within PalB are schematized. MIT, microtubule interacting and trafficking domain (11, 59, 61, 71); Calpain_II, calpain domain II; PalBh, PalB homologous domain; Calpain_III, Calpain large subunit domain III

4°C and revealed with peroxidase-conjugated goat anti-mouse immunoglobulin G (IgG) (heavy plus light chains) (Jackson ImmunoResearch Laboratories) used at a 1/4,000 dilution. PalB::HA_3 was detected with rat monoclonal 3F10 primary antibody (Roche) used at a 1/1,000 dilution and revealed with peroxidase-coupled goat anti-rat IgG plus IgM from Southern Biotech at a 1/4,000 dilution. Actin was detected with mouse anti-actin (1/5,000, clone C4; ICN Biomedicals, Inc.) and revealed as MYC3::PacC. Peroxidase activity was visualized using ECL detection reagents (G E Healthcare). The PalB::HA_3 allele (Eliecer Díez and M. Á. Peñalva, unpublished) will be described elsewhere.

RESULTS AND DISCUSSION

Mutational analysis of the candidate signaling protease gene, *palB*. To characterize further the putative signaling protease, we carried out a mutational analysis of *palB*. The majority of *palB* mutations analyzed in this work (Table 2) were obtained by exploiting the powerful GABA technique (1, 15, 24, 42, 46). The selection relies on the ability of loss-of-function mutations in any of the *pal* genes and *pacC* to suppress *areA*^{r} (= *areA*$^-$, nitrogen metabolite repressed) mutations for growth on GABA as the sole nitrogen source in the presence of glucose as the carbon source. The suppression occurs through the derepression of the acid-expressed *gabA* gene, which specifies the GABA permease, by largely preventing formation of PacC^{27}, the acid-expressed gene repressor. In haploid strains, suppressor mutations can arise in *pacC* and in any of the *pal* genes. In diploid strains homozygous for *areA*^{r} and containing one wild-type and one mutant copy of the *pal* gene of interest, suppressor mutations are targeted to this particular *pal* gene, as described in detail by Tilburn et al. (68). Mutations described here were also tested for their effects on other pH characteristics. These effects are described in detail elsewhere (7, 69). Briefly, and as relevant here, loss-of-function mutations in *pacC* and any of the *pal* genes mimic the effects of growth under acidic conditions. They have elevated, derepressed levels of acid-expressed acid phosphatase. They are also molybdate hypersensitive and aminoglycoside resistant due to molybdate toxicity being greatest and aminoglycoside potency least in acidic medium. In addition, because they are unable to respond to alkalinity, they are alkali sensitive. Since alkali sensitivity, assayed by growth on pH-8 medium, is the most sensitive test, the severity of mutations was assessed by the abilities of the respective mutants to grow on pH-8 medium.

Characterization of *palB* alleles identifies mutations affecting the catalytic domain, a potential regulatory domain, and the C-terminal region. Twenty-seven *palB* mutations, including nine missense and eighteen truncating mutations, were characterized (Table 2; Fig. 3). Three of the missense mutations occur in the catalytic domain (Fig. 3) (cd00044 [41] at http://www.ncbi.nlm.nih.gov/). *palB517*(*D197E C198F*) contains a null double mutation affecting the predicted, essential, and invariant cysteine of the catalytic triad. Aspartate or asparagine (14) occupies the position corresponding to Asp197 in all 36 protein representatives of cd00044. *palB16*(*V200N*) substitutes a conserved hydrophobic residue (in the fungal PalBs and cd00044 representatives) in very close proximity to the predicted catalytic cysteine, with polar asparagine, resulting in a complete loss of function. The phenotypes of *palB517* and *palB16* highlight the importance of the predicted catalytic cysteine and its environment and strongly support the deduction that PalB is, in fact, a cysteine protease. *palB504*(*L307R*) occurs between, in the primary structure, the catalytic cysteine and the other active-site residues His366 and Asn386, affecting a highly conserved hydrophobic residue. In alignment with human *m*-calpain (shown in part in Fig. 3), Leu307 occurs between two partially conserved glycine pairs, the first of which is important in substrate binding and the second in providing a hinge (32, 57, 65).

In the PalB C terminus (Fig. 3) the *palB111* mutation truncating the protein after Val766 is the most C-terminal null mutation. *palB7* and *palB37*, truncating the protein after Ser790 and Leu813, respectively, do not reduce mRNA stability (43) and are very slightly functional at low temperature. These phenotypes indicate that structurally or functionally essential residues are located between Val766 and Ser790 and that very important, but not strictly essential, residues occur C-terminal to Leu813 in the last ~4% of the protein.

Sequence similarity and mutational analysis described here strongly support the view that PalB is a calpain-like cysteine protease. Since calpains are regulatory proteases which cleave between regulatory domains, this favors PalB as the signaling protease which removes the negatively acting PacC C terminus. However, we cannot exclude the possibility that the phenotypes of any *palB* mutations characterized here might result from reduced PalB protein levels rather than impaired PalB function. This could be due to protein or even messenger instability, except in the cases of *palB7* and *palB37*, where the latter possibility has been excluded (43).

Is PalB posttranscriptionally pH regulated? It has been reported previously that *palB* transcript levels are not pH reg-

(16, 25, 26, 32, 57, 65, 66; for a review, see reference 63). Stars highlight the positions of the catalytic triad residues, cysteine, histidine, and asparagine/aspartate. The conserved regions around the catalytic triad residues, cysteine (residues 191 to 202) and histidine and asparagine/aspartate (residues 361 to 388), and conserved and rather poorly conserved regions around Leu307Arg (residues 300 to 313) and Ile618Leu and Ser619Pro (612 to 622), respectively, are shown above the scheme. Missense and truncating mutations in the C terminus (residues 700 to 847) are shown below the scheme. Residue changes and truncating mutations are indicated with upward- and downward-pointing arrows, respectively. Null mutations are indicated with solid-headed arrows, and those retaining some function are indicated with open-headed arrows. Abbreviations and accession numbers (emb, EMBL; sp, SwissProt; up, UniProt) are as follows: An, *A. nidulans*, emb Z54244; Ci, *Coccidioides immitis*, up Q1DXZ5; Hc, *Histoplasma capsulatum*, retranslated from sequence from locus HCAG_04795.1 (http://www.broad.mit.edu/annotation/genome/histoplasma_capsulatum/); Chg, *Chaetomium globosum*, up Q2H9W2; Nc, *Neurospora crassa*, sp Q7RZP7; Gz, *Gibberella zeae*, up Q4IBM8; Phn, *Phaesophaeria nodorum*, up Q0U7L9; Cn, *Cryptococcus neoformans*, sp Q55IT8; Um, *Ustilago maydis*, up Q4PCT8; Yl, *Yarrowia lipolytica*, sp Q9HFC8; Ca, *Candida albicans*, sp Q5AK25; Dh, *Debaromyces hansenii*, Q6BH66; Ag, *Ashbya gossipii*, Q759K3; Kl, *Kluyveromyces lactis*, sp Q6CKY3; Cg, *Candida glabrata*, Q6FJ28; Sc, *S. cerevisiae*, Q03792; m-c, human *m*-calpain, sp Q17655. Residues removed from the *C. globosum* and *N. crassa* sequences are (−25) VGRGGGGSGGESSGGGGGGSAVRVSLEVG and (−49) IEGRKRVLASTASGGGGELAASLSNLSLSERLGGIGGI GGGHIHG, respectively, as indicated. Shading is according to Blosom 62 similarity groups (DN, EQ, KR, ST, ILMV, and FYW): 50% similar, black; 40% similar, dark gray; 30% similar, light gray.

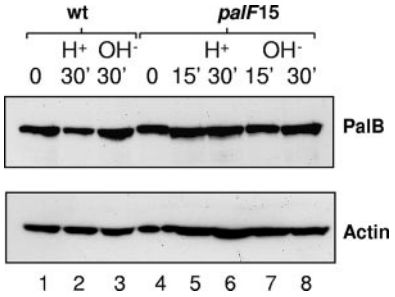

FIG. 4. PalB protein levels are not pH regulated. Western blot analysis of HA_3-tagged PalB in *palF*$^+$ and *palF15* cells which were grown in acidic medium (H^+) and harvested, indicated by "0" above the lane, or shifted to acidic or alkaline (OH^-) medium for 15 or 30 min, as indicated above the lane. Actin loading controls were obtained from a Western blot of a duplicate gel.

ulated (16). However, since signaling proteolysis occurs strictly in response to alkaline ambient pH, presuming that PalB is the signaling protease, it is also relevant to determine whether PalB protein levels are pH dependent and if PalB is posttranslationally modified in a pH-dependent fashion. To do this, we used an HA_3-tagged *palB* strain, which is wild type for all pH characteristics tested (results not shown), and followed C-terminally HA_3-tagged PalB in Western blots following a shift from acidic medium to alkaline medium. (Note that C-terminal truncations removing the HA_3 tag and small N-terminal truncations below the resolution of the gel would not be detectable). There was no change in PalB levels 30 min after shifting (Fig. 4, lanes 1 and 3). PalB levels were similar under similar growth conditions in a *palF15* (loss-of-function [30]) strain (Fig. 4, compare lanes 1 and 4, 2 and 6, and 3 and 8). PalB levels were also unaffected by *palC4*, *palA1*, *palH17*, and *palI32* loss-of-function mutations (data not shown). Furthermore, there are no detectable pH-associated changes in mobility, which would indicate certain posttranslational modifications. However, these results cannot exclude the possible occurrence of posttranslational modifications not affecting mobility or beyond detection under the experimental conditions employed here.

These results suggest that de novo synthesis of PalB is not required for signaling proteolysis, which occurs within 15 min after shifting to alkaline growth medium (17) (Fig. 5 and 8). However, the possibility of de novo synthesis coupled with increased turnover cannot be excluded.

MYC_3-tagged *pacC*. To facilitate the analysis of PacC signaling proteolysis in Western blots, we used a strain containing the *pacC900* (MYC_3-tagged *pacC*) allele obtained by gene replacement as described in the Materials and Methods and Fig. 2. The strain was fully characterized for pH characteristics in crosses and was found to be indistinguishable from untagged wild-type strains, as shown for certain pH characteristics in Fig. 7).

PalB is essential for the signaling proteolysis but irrelevant for processing proteolysis. With newly acquired tools, namely null *palB* alleles and wild-type MYC_3-tagged PacC, at our disposal, we decided to review the role of PalB in PacC processing. To do this, we also took into account the transient nature of the $PacC^{53}$ form and followed PacC processing in response to shifting to alkaline ambient pH (processing triggering conditions). In a wild-type strain (*palB*$^+$; MYC-tagged *pacC*$^+$ [*pacC900*]), $PacC^{72}$ is progressively converted to $PacC^{27}$ via the $PacC^{53}$ product of signaling proteolysis within 2 h of shifting from acidic to alkaline growth conditions (Fig. 5A, lanes 1 to 5). This conversion is completely prevented in the null *palB38* strain (Fig. 5A, lanes 6 to 10), in which PalB is truncated after residue 54 (Table 2), removing ~94% of the protein, including the entire catalytic domain (Fig. 3). Figure 5B shows that wild-type $PacC^{72}$ remains unprocessed in the absence of PalB even after prolonged culture (16 h) under alkaline conditions (Fig. 5B, lanes 3 and 4). In contrast, in the *pacC*^{c}*14* strain, where the PacC protein is truncated at residue 492, within the signaling protease box (17, 69) and approximating the physiological cleavage site (within residues 493 to 500), PacC is processed irrespective of the pH of the growth medium and the functionality of PalB (Fig. 5B, lanes 5 to 8).

This experiment confirms the results of similar but earlier and consequently less rigorous experiments (16, 17). Both experiments relied on the extant *palB7* allele, which here we show to be a small C-terminal truncation which retains a small amount of function (Table 2; Fig. 3). While the former (16) demonstrated that PacC processing which is prevented by the

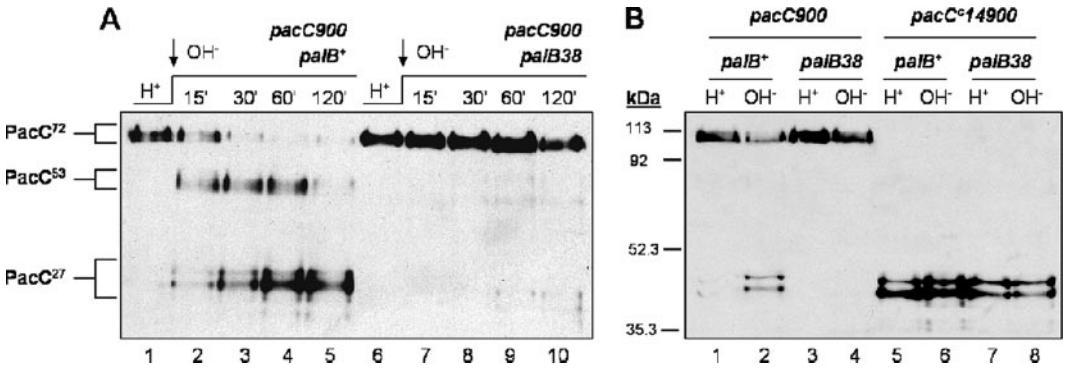

FIG. 5. PalB is required for signaling proteolysis but not processing proteolysis of PacC. Western blot analysis of MYC_3-tagged PacC processing in *palB*$^+$ and *palB38* strains (A) grown under acidic conditions and shifted to alkaline conditions for the times indicated above the panel or (B) grown under steady-state acidic or alkaline conditions, as indicated, with MYC_3-tagged $PacC^c14$ (Y493stop), where PacC is mutationally truncated within the signaling protease box. There is some heterogeneity at the C terminus of $PacC^{27}$ (42).

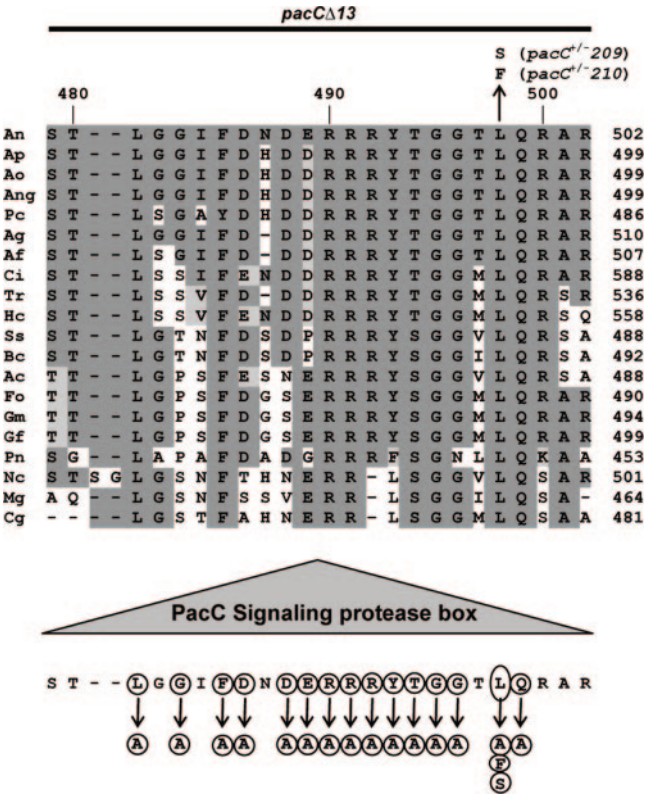

FIG. 6. Conservation of the PacC signaling protease box. Interspecies alignment shows conserved residues in the region of the 24-residue signaling protease box described by Díez et al. (17). Identical or similar (Ser/Thr, Iso/Val, Asp/Glu, Phe/Tyr, and Arg/Lys) residues are highlighted in dark or light gray, respectively. Abbreviations and accession numbers (Chg, *Chaetomium globosum* database at http://www.broad.mit.edu/annotation/genome/chaetomium_globosum/; dbj, DNA Data Base Japan; emb, EMBL; gb, GenBank; sp, SwissProt; up, UniPro) are as follows: An, *A. nidulans*, emb Z47081.1; Ap, *Aspergillus parasiticum*, gb AAK98616.1; Ao, *Aspergillus oryzae*, dbj BAE57899.1; Ang, *Aspergillus niger*, emb CAA67063; Pc, *Penicillium chrysogenum*, gb AAC36492.1; Ag, *Aspergillus giganteus*, gb AAV28549.1; Af, *Aspergillus fumigatus*, sp Q4WY67; Ci, *Coccidioides immitis*, gb EAS32701.1; Tr, *Trichophyton rubrum*, gb AAK35072.2; Hc, *Histoplasma capsulatum*, sp Q52B93; Ss, *Sclerotinia sclerotium*, sp Q9P413; Bf, *Botryotinia fuckeliana*, gb AAV54519.1; Ac, *Acremonium chrysogenum*, spQ96X49; Fo, *Fusarium oxysporum*, sp Q870A3; Gm, *Gibberella moniformis*, sp Q873X0; Gf, *Gibberella fujikuroi*, sp Q8J1U9; Pn, *Phaeosphaeria nodorum*, gb EAT80783.1; Nc, *Neurospora crassa*, sp Q7RVQ8; Mg, *Magnaportha grisea*, sp Q52B93; Cg, *Chaetomium globosum*, Chg CHGG_05804.1. *A. nidulans* PacC amino acid numbers (69) and consequences of the *pacCΔ13* deletion and classically derived $pacC^{+/-}209$ and $pacC^{+/-}210$ mutations (17) are shown above the alignment. Residues mutated in MYC-tagged PacC in this work are presented below the alignment.

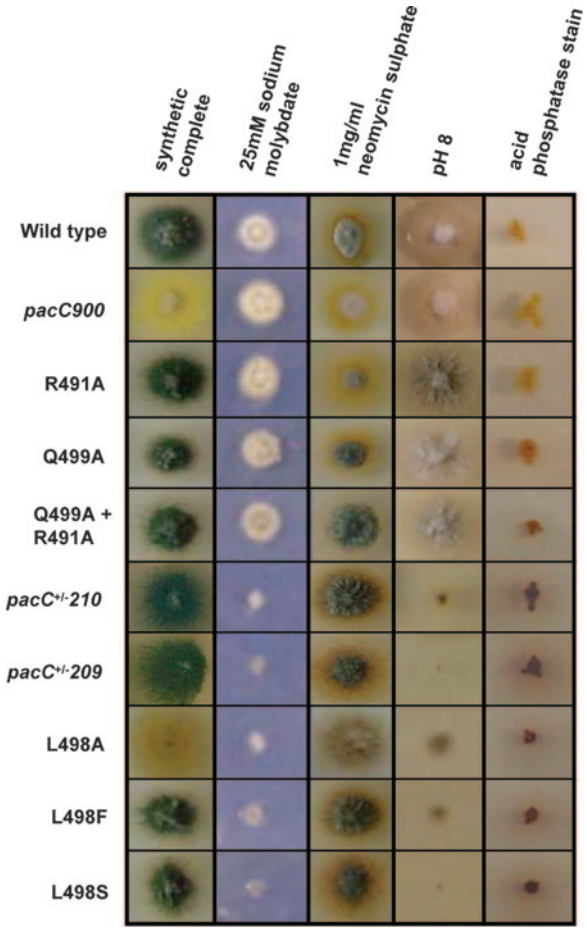

FIG. 7. Phenotype testing of signaling protease box mutants in plate tests. The wild-type strain in row 1 is an untagged *biA1* (biotin-requiring) strain. The difference in colony color on synthetic complete or neomycin-containing medium is due to differently pigmented (green or yellow) conidia and has no effect on pH characteristics. Acid phosphatase staining was carried out after growth on pH-8 minus-phosphate medium.

palB7 mutation occurs constitutively in a strain also carrying the more severe (than $pacC^{c}14$) mutation $pacC^{c}202$ (69), it was performed prior to the conception of two-step proteolysis and thus was not designed to address the role of PalB in the signaling proteolysis step. The latter (17) relied upon deletion of the PacC processing efficiency determinant to allow detection of the transient and untagged PacC intermediate form and demonstrated that the *palB7* mutation prevents the formation of a mutant PacC intermediate form lacking residues 169 to 407 (17). The experiment described here clearly demonstrates that while PalB is not required for conversion of $PacC^{53}$ to $PacC^{27}$, it is definitely required for conversion of $PacC^{72}$ to $PacC^{53}$, consistent with its being the signaling protease.

Alanine scanning mutagenesis of the PacC signaling protease box. Having confirmed the suitability of PalB as the signaling protease, we turned to the further characterization of the substrate PacC, where we had previously identified a conserved sequence in the cleavage region (17). Figure 6 shows a recent interspecies alignment of the putative signaling protease box region of PacCs obtained by similarity searches of the databases. This supports our former conclusion that there is a conspicuously high level of conservation in this region, and it is remarkable that all of the 19 sequences are from euascomycetes. Notably, we have been unable to identify similar regions in any hemiascomycetous Rim101s despite the predicted conservation in function between Rim13p and PalB. To characterize further this region with respect to its relevance in signaling proteolysis, we carried out a mutational analysis, replacing different amino acids within the 24-residue conserved "signaling protease box" (17) of MYC_3-tagged PacC (designated

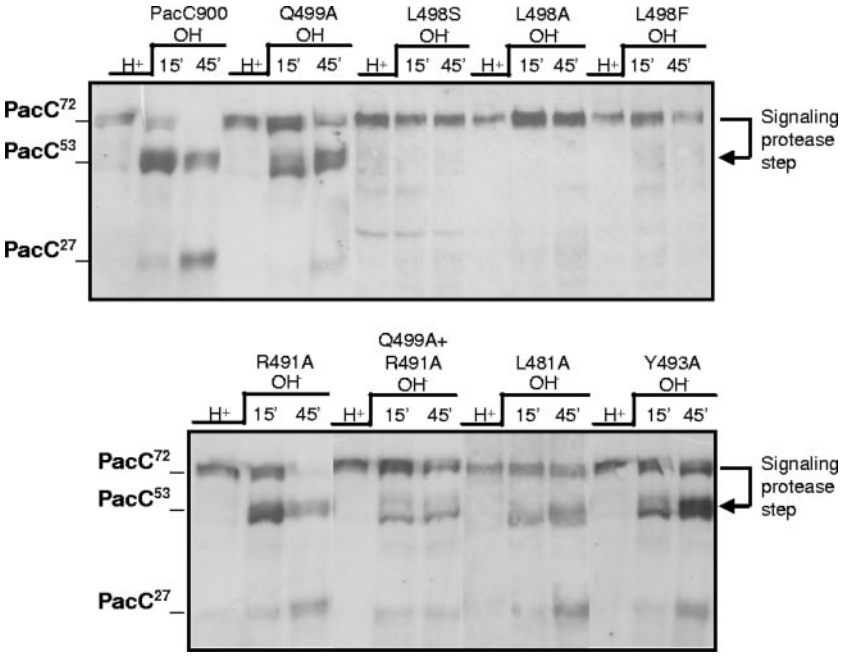

FIG. 8. Western blot analysis of PacC forms in signaling protease box mutants in response to shifting from acidic to alkaline growth medium. The positions of the PacC forms are indicated on the left.

pacC900) with alanine residues. We focused on 15 of the most highly conserved residues, and we also prepared MYC_3-tagged versions of the classically obtained *pacC*$^{+/-}$*209* and *pacC*$^{+/-}$*210* (17), *pacC900*(*L498S*), and *pacC*900(*L498F*), respectively. The substitutions are summarized in Fig. 6 and the methodology schematized in Fig. 2.

Phenotypic analysis in plate tests of *pacC* mutations affecting the signaling protease box (Fig. 7). *pacC900*(*L498S*) and *pacC*$^{+/-}$*209*(*L498S*) strains had a loss-of-function, acidity-mimicking phenotype (Fig. 7), virtually indistinguishable from that seen with null mutations in the *palA*, *palB*, *palC*, *palF*, and *palH* genes (data not shown). The mutants failed to germinate on pH-8 medium; they were molybdate hypersensitive and neomycin resistant and had derepressed levels of acid phosphatase activity relative to wild-type (*pacC900* or untagged) controls. *pacC900*(*L498F*) and *pacC*$^{+/-}$*210*(*L498F*) strains were slightly leaky and the *pacC900*(*L498A*) strain a little more so, showing very small amounts of growth on pH 8.0 medium. The other alanine substitutions depicted in Fig. 6 resulted in phenotypes virtually indistinguishable from that of wild-type strains in plate tests, apart from *pacC900*(*Q499A*) and the double mutation *pacC900*(*R491A Q499A*), which resulted in slight neomycin resistance and acid phosphatase derepression (Fig. 7). The *pacC900*(*R491A*) single mutation had no identifiable mutant phenotype by itself but appeared to augment *pacC900*(*Q499A*) neomycin resistance and acid phosphatase derepression in the double mutant.

Western blot analysis of PacC processing in signaling protease box mutants in response to pH shifting. In view of the extremely subtle phenotypes of the *pacC900*(*Q499A*) and *pacC900*(*R491A Q499A*) alleles in plate tests, we chose to use a more sensitive procedure whereby PacC processing after shifting from acidic to alkaline medium was followed over 45 min by Western analysis (Fig. 8). This gives a qualitative indication of the rate of signaling proteolysis by the rate of disappearance of the PacC^{72} form. In the nonsubstituted *pacC900* strain, used as wild-type control, and the *pacC900*(*R491A*) strain, PacC^{72} was converted to PacC^{53} and PacC^{27} after a shift to alkaline conditions for 45 min. In stark contrast, PacC^{72} remained essentially unprocessed in mutants containing the L498S, L498F, and L498A substitutions. *pacC900*(*L481A*), *pacC900*(*Y493A*), *pacC900*(*Q499A*), and *pacC900*(*Q499A R491A*) strains had intermediate phenotypes, with conspicuous amounts of PacC^{72} persisting after 45 min, which showed incomplete conversion of the PacC^{72} form of the mutant proteins to their intermediate PacC^{53} and processed PacC^{27} forms. The *pacC900*(*R491A*) single-mutant strain behaved like the wild type in Western blots, as in plate tests, and appeared to further reduce levels of PacC^{53} relative to those of PacC^{72} after shifting to alkaline conditions when combined with the Q499A substitution in the *pacC900*(*R491A Q499A*) strain.

In this Western blot analysis, the extent to which PacC^{72} proteolysis was delayed approximately reflected the degree of acidity mimicry shown in plate tests. Strains containing substitutions L481A and Y493A, which resulted in virtually wild-type phenotypes in plate tests, were slightly delayed in PacC processing, with some PacC^{72} remaining after 45 min, and had reduced but appreciable levels of PacC^{27}. Strains containing Q499A and R491A Q499A, which resulted in marginal loss-of-function phenotypes in plate tests, also had considerable amounts of PacC^{72} and even less PacC^{27} after 45 min. The reduced levels of the processed form could be accounted for by a reduced rate of substrate PacC^{53} production due to impaired signaling proteolysis. However, we cannot exclude the possibility that the reduced levels of processed PacC^{27} are due, at least in part, to impaired processing proteolysis. This is partic-

ularly possible in the *pacC900*(*R491A Q499A*) double mutant, where R491A occurs within the $PacC^{53}$ moiety, and where $PacC^{27}$ levels are particularly low after 45 min.

Signaling proteolysis resembles calpain cleavage. Mutational analysis of the signaling protease box clearly indicates that excepting Leu498, the primary structure of this region contains no residues stringently required by the signaling protease; rather, there are sequence preferences. This reflects the situation with calpain substrates, where the determinants of cleavage specificity have been highly debated and somewhat elusive. However, in a relatively recent and comprehensive study, Tompa et al. (70) analyzed 106 *m*- or μ-calpain cleavage sites in 49 substrates and found that there were amino acid preferences extending from P4 to P7′ around the scissile bond, a somewhat narrower span than that of the 19 within the signaling protease region examined here. They also found that there are secondary structural features and PEST-like sequences in the region of the scissile bonds, suggesting that calpain cleaves rather disorganized protein segments. We failed to find a PEST-like sequence in the close vicinity of the signaling protease box, but the core of the *A. nidulans* signaling protease box from Thr480 to Arg500 is flanked N-terminally by a 9-residue sequence and C-terminally by an 11-residue sequence of low complexity (SEG low-complexity region) (77), identified using the PredictProtein server (http://predictprotein.org/ [58]).

These studies support the prediction that PalB is a calpain-like cysteine protease and that PacC is an appropriate calpain substrate, strongly buttressing the contention that PalB is the obvious candidate for the signaling protease. The lack of sequence requirement in the PacC cleavage site and the pH independence of PalB protein levels beg the questions of how the specificity and pH regulation of signaling proteolysis are achieved. It seems possible that the answers lie in PalA. PalA binding of PacC through YPXL/I motif(s) is essential (73), and it is tempting to speculate that the way in which PalA positions PacC with respect to PalB on endosomal membranes determines the cleavage site, as suggested for *S. cerevisiae* (78). Perhaps all that is needed is a cleavable scissile bond in the right place. This would allow pH regulation of signaling proteolysis through the pH-dependent localization of Rim20p/PalA to Vps32-containing endosomal membranes as recently demonstrated for *S. cerevisiae* (6). We cannot, however, ignore the possibility that PalB localization and/or activation is also pH dependent, and this remains an area for future study.

ACKNOWLEDGMENTS

We are grateful to Eduardo A. Espeso for the kind gift of the *palB70* strain and for critically reading the manuscript. Helpful suggestions were also made by three anonymous reviewers. We thank Eliecer Díez for supplying the tagged *palB* allele.

This work was supported by Wellcome Trust grant 067878 to H.N.A. and J.T. and DGICYT BIO2006-00556 to M.A.P.; M.M.P. was a recipient of a postdoctoral fellowship from the Ministerio de Educación y Ciencia (Spain).

REFERENCES

1. **Arst, H. N., Jr., E. Bignell, and J. Tilburn.** 1994. Two new genes involved in signalling ambient pH in *Aspergillus nidulans*. Mol. Gen. Genet. **245:**787–790.
2. **Arst, H. N., Jr., and M. Á. Peñalva.** 2003. pH regulation in *Aspergillus* and parallels with higher eukaryotic regulatory systems. Trends Genet. **19:**224–231.
3. **Aza-Blanc, P., F. A. Ramirez-Weber, M. P. Laget, C. Schwartz, and T. B. Kornberg.** 1997. Proteolysis that is inhibited by hedgehog targets Cubitus interruptus protein to the nucleus and converts it to a repressor. Cell **89:**1043–1053.
4. **Barwell, K. J., J. H. Boysen, W. Xu, and A. P. Mitchell.** 2005. Relationship of *DFG16* to the Rim101p pH response pathway in *Saccharomyces cerevisiae* and *Candida albicans*. Eukaryot. Cell **4:**890–899.
5. **Betts, J. C., and G. J. Nabel.** 1996. Differential regulation of NF-κB2(p100) processing and control by amino-terminal sequences. Mol. Cell. Biol. **16:**6363–6371.
6. **Boysen, J. H., and A. P. Mitchell.** 2006. Control of Bro1-domain protein Rim20 localization by external pH, ESCRT machinery, and the *Saccharomyces cerevisiae* Rim101 pathway. Mol. Biol. Cell **17:**1344–1353.
7. **Brown, M. S., J. Ye, R. B. Rawson, and J. L. Goldstein.** 2000. Regulated intramembrane proteolysis: a control mechanism conserved from bacteria to humans. Cell **100:**391–398.
8. **Caddick, M. X., A. G. Brownlee, and H. N. Arst, Jr.** 1986. Regulation of gene expression by pH of the growth medium in *Aspergillus nidulans*. Mol. Gen. Genet. **203:**346–353.
9. **Carafoli, E., and M. Molinari.** 1998. Calpain: a protease in search of a function? Biochem. Biophys. Res. Commun. **247:**193–203.
10. **Chen, C. H., D. P. von Kessler, W. Park, B. Wang, Y. Ma, and P. A. Beachy.** 1999. Nuclear trafficking of Cubitus interruptus in the transcriptional regulation of Hedgehog target gene expression. Cell **98:**305–316.
11. **Ciccarelli, F. D., C. Proukakis, H. Patel, H. Cross, S. Azam, M. A. Patton, P. Bork, and A. H. Crosby.** 2003. The identification of a conserved domain in both spartin and spastin, mutated in hereditary spastic paraplegia. Genomics **81:**437–441.
12. **Clutterbuck, A. J.** 1993. *Aspergillus nidulans*, p. 3.71–3.84. *In* S. J. O'Brien (ed.), Genetic maps. Locus maps of complex genomes, 6th ed., vol. 3. Cold Spring Harbor Laboratory Press, Cold Spring Harbor, NY.
13. **Cove, D. J.** 1966. The induction and repression of nitrate reductase in the fungus *Aspergillus nidulans*. Biochim. Biophys. Acta **113:**51–56.
14. **Dear, N., K. Matena, M. Vingron, and T. Boehm.** 1997. A new subfamily of vertebrate calpains lacking a calmodulin-like domain: implications for calpain regulation and evolution. Genomics **45:**175–184.
15. **Denison, S. H., S. Negrete-Urtasun, J. M. Mingot, J. Tilburn, W. A. Mayer, A. Goel, E. A. Espeso, M. Á. Peñalva, and H. N. Arst, Jr.** 1998. Putative membrane components of signal transduction pathways for ambient pH regulation in *Aspergillus* and meiosis in *Saccharomyces* are homologous. Mol. Microbiol. **30:**259–264.
16. **Denison, S. H., M. Orejas, and H. N. Arst, Jr.** 1995. Signaling of ambient pH in *Aspergillus* involves a cysteine protease. J. Biol. Chem. **270:**28519–28522.
17. **Díez, E., J. Álvaro, E. A. Espeso, L. Rainbow, T. Suárez, J. Tilburn, H. N. Arst, Jr., and M. Á. Peñalva.** 2002. Activation of the *Aspergillus* PacC zinc finger transcription factor requires two proteolytic steps. EMBO J. **21:**1350–1359.
18. **Dorn, G.** 1965. Genetic analysis of the phosphatases in *Aspergillus nidulans*. Genet. Res. **6:**13–26.
19. **Espeso, E. A., and H. N. Arst, Jr.** 2000. On the mechanism by which alkaline pH prevents expression of an acid-expressed gene. Mol. Cell. Biol. **20:**3355–3363.
20. **Espeso, E. A., and M. Á. Peñalva.** 1996. Three binding sites for the *Aspergillus nidulans* PacC zinc-finger transcription factor are necessary and sufficient for regulation by ambient pH of the isopenicillin N synthase gene promoter. J. Biol. Chem. **271:**28825–28830.
21. **Espeso, E. A., T. Roncal, E. Díez, L. Rainbow, E. Bignell, J. Álvaro, T. Suárez, S. H. Denison, J. Tilburn, H. N. Arst, Jr., and M. Á. Peñalva.** 2000. On how a transcription factor can avoid its proteolytic activation in the absence of signal transduction. EMBO J. **19:**719–728.
22. **Espeso, E. A., J. Tilburn, L. Sanchez-Pulido, C. V. Brown, A. Valencia, H. N. Arst, Jr., and M. Á. Peñalva.** 1997. Specific DNA recognition by the *Aspergillus nidulans* three zinc finger transcription factor PacC. J. Mol. Biol. **274:**466–480.
23. **Fan, C. M., and T. Maniatis.** 1991. Generation of p50 subunit of NF-κB by processing of p105 through an ATP-dependent pathway. Nature **354:**395–398.
24. **Fernández-Martínez, J., C. V. Brown, E. Díez, J. Tilburn, H. N. Arst, Jr., M. Á. Peñalva, and E. A. Espeso.** 2003. Overlap of nuclear localisation signal and specific DNA-binding residues within the zinc finger domain of PacC. J. Mol. Biol. **334:**667–684.
25. **Fernández-Montalvan, A., I. Assfalg-Machleidt, D. Pfeiler, H. Fritz, M. Jochum, and W. Machleidt.** 2004. Electrostatic interactions of domain III stabilize the inactive conformation of μ-calpain. Biochem. J. **382:**607–617.
26. **Futai, E., T. Kubo, H. Sorimachi, K. Suzuki, and T. Maeda.** 2001. Molecular cloning of PalBH, a mammalian homologue of the *Aspergillus* atypical calpain PalB. Biochim. Biophys. Acta **1517:**316–319.
27. **Goulet, B., and A. Nepveu.** 2004. Complete and limited proteolysis in cell cycle progression. Cell Cycle **3:**986–989.
28. **Goulet, B., M. Truscott, and A. Nepveu.** 2006. A novel proteolytically processed CDP/Cux isoform of 90 kDa is generated by cathepsin L. Biol. Chem. **387:**1285–1293.

29. **Hayashi, M., T. Fukuzawa, H. Sorimachi, and T. Maeda.** 2005. Constitutive activation of the pH-responsive Rim101 pathway in yeast mutants defective in late steps of the MVB/ESCRT pathway. Mol. Cell. Biol. **25:**9478–9490.
30. **Herranz, S., J. M. Rodríguez, H. J. Bussink, J. C. Sánchez-Ferrero, H. N. Arst, Jr., M. Á. Peñalva, and O. Vincent.** 2005. Arrestin-related proteins mediate pH signaling in fungi. Proc. Natl. Acad. Sci. USA **102:**12141–12146.
31. **Hoppe, T., K. Matuschewski, M. Rape, S. Schlenker, H. D. Ulrich, and S. Jentsch.** 2000. Activation of a membrane-bound transcription factor by regulated ubiquitin/proteasome-dependent processing. Cell **102:**577–586.
32. **Hosfield, C. M., J. S. Elce, P. L. Davies, and Z. Jia.** 1999. Crystal structure of calpain reveals the structural basis for Ca(2+)-dependent protease activity and a novel mode of enzyme activation. EMBO J. **18:**6880–6889.
33. **Ito, T., T. Chiba, R. Ozawa, M. Yoshida, M. Hattori, and Y. Sakaki.** 2001. A comprehensive two-hybrid analysis to explore the yeast protein interactome. Proc. Natl. Acad. Sci. USA **98:**4569–4574.
34. **Katoh, K., H. Shibata, K. Hatta, and M. Maki.** 2004. CHMP4b is a major binding partner of the ALG-2-interacting protein Alix among the three CHMP4 isoforms. Arch. Biochem. Biophys. **421:**159–165.
35. **Katoh, K., H. Shibata, H. Suzuki, A. Nara, K. Ishidoh, E. Kominami, T. Yoshimori, and M. Maki.** 2003. The ALG-2-interacting protein Alix associates with CHMP4b, a human homologue of yeast Snf7 that is involved in multivesicular body sorting. J. Biol. Chem. **278:**39104–39113.
36. **Kim, J., S. Sitaraman, A. Hierro, B. M. Beach, G. Odorizzi, and J. H. Hurley.** 2005. Structural basis for endosomal targeting by the Bro1 domain. Dev. Cell **8:**937–947.
37. **Lamb, T. M., W. Xu, A. Diamond, and A. P. Mitchell.** 2001. Alkaline response genes of *Saccharomyces cerevisiae* and their relationship to the RIM101 pathway. J. Biol. Chem. **276:**1850–1856.
38. **Li, W., and A. P. Mitchell.** 1997. Proteolytic activation of Rim1p, a positive regulator of yeast sporulation and invasive growth. Genetics **145:**63–73.
39. **Maccheroni, W., Jr., G. S. May, N. M. Martinez-Rossi, and A. Rossi.** 1997. The sequence of *palF*, an environmental pH response gene in *Aspergillus nidulans*. Gene **194:**163–167.
40. **Makinoshima, H., and M. S. Glickman.** 2006. Site-2 proteases in prokaryotes: regulated intramembrane proteolysis expands to microbial pathogenesis. Microbes Infect. **8:**1882–1888.
41. **Marchler-Bauer, A., and S. H. Bryant.** 2004. CD-Search: protein domain annotations on the fly. Nucleic Acids Res. **32:**W327–W331.
42. **Mingot, J. M., J. Tilburn, E. Díez, E. Bignell, M. Orejas, D. A. Widdick, S. Sarkar, C. V. Brown, M. X. Caddick, E. A. Espeso, H. N. Arst, Jr., and M. Á. Peñalva.** 1999. Specificity determinants of proteolytic processing of *Aspergillus* PacC transcription factor are remote from the processing site, and processing occurs in yeast if pH signalling is bypassed. Mol. Cell. Biol. **19:**1390–1400.
43. **Morozov, I. Y., S. Negrete-Urtasun, J. Tilburn, C. A. Jansen, M. X. Caddick, and H. N. Arst, Jr.** 2006. Nonsense-mediated mRNA decay mutation in *Aspergillus nidulans*. Eukaryot. Cell **5:**1838–1846.
44. **Munro, S., and H. R. Pelham.** 1986. An Hsp70-like protein in the ER: identity with the 78 kd glucose-regulated protein and immunoglobulin heavy chain binding protein. Cell **46:**291–300.
45. **Negrete-Urtasun, S., S. H. Denison, and H. N. Arst, Jr.** 1997. Characterization of the pH signal transduction pathway gene *palA* of *Aspergillus nidulans* and identification of possible homologs. J. Bacteriol. **179:**1832–1835.
46. **Negrete-Urtasun, S., W. Reiter, E. Díez, S. H. Denison, J. Tilburn, E. A. Espeso, M. Á. Peñalva, and H. N. Arst, Jr.** 1999. Ambient pH signal transduction in *Aspergillus*: completion of gene characterization. Mol. Microbiol. **33:**994–1003.
47. **Nickas, M. E., and M. P. Yaffe.** 1996. *BRO1*, a novel gene that interacts with components of the Pkc1p-mitogen-activated protein kinase pathway in *Saccharomyces cerevisiae*. Mol. Cell. Biol. **16:**2585–2593.
48. **Orejas, M., E. A. Espeso, J. Tilburn, S. Sarkar, H. N. Arst, Jr., and M. Á. Peñalva.** 1995. Activation of the *Aspergillus* PacC transcription factor in response to alkaline ambient pH requires proteolysis of the carboxy-terminal moiety. Genes Dev. **9:**1622–1632.
49. **Palombella, V. J., O. J. Rando, A. L. Goldberg, and T. Maniatis.** 1994. The ubiquitin-proteasome pathway is required for processing the NF-κB1 precursor protein and the activation of NF-κB. Cell **78:**773–785.
50. **Pan, Y., C. B. Bai, A. L. Joyner, and B. Wang.** 2006. Sonic hedgehog signaling regulates Gli2 transcriptional activity by suppressing its processing and degradation. Mol. Cell. Biol. **26:**3365–3377.
51. **Peck, J. W., E. T. Bowden, and P. D. Burbelo.** 2004. Structure and function of human Vps20 and Snf7 proteins. Biochem. J. **377:**693–700.
52. **Peñalva, M. Á., and H. N. Arst, Jr.** 2002. Regulation of gene expression by ambient pH in filamentous fungi and yeasts. Microbiol. Mol. Biol. Rev. **66:**426–446.
53. **Peñalva, M. Á., and H. N. Arst, Jr.** 2004. Recent advances in the characterization of ambient pH regulation of gene expression in filamentous fungi and yeasts. Annu. Rev. Microbiol. **58:**425–451.
54. **Price, M. A., and D. Kalderon.** 2002. Proteolysis of the Hedgehog signaling effector Cubitus interruptus requires phosphorylation by glycogen synthase kinase 3 and casein kinase 1. Cell **108:**823–835.
55. **Rape, M., and S. Jentsch.** 2002. Taking a bite: proteasomal protein processing. Nat. Cell Biol. **4:**E113–E116.
56. **Rape, M., and S. Jentsch.** 2004. Productive RUPture: activation of transcription factors by proteasomal processing. Biochim. Biophys. Acta **1695:**209–213.
57. **Reverter, D., S. Strobl, C. Fernandez-Catalan, H. Sorimachi, K. Suzuki, and W. Bode.** 2001. Structural basis for possible calcium-induced activation mechanisms of calpains. Biol. Chem. **382:**753–766.
58. **Rost, B., G. Yachdav, and J. Liu.** 2004. The PredictProtein server. Nucleic Acids Res. **32:**W321–W326.
59. **Scheuring, S., R. A. Röhricht, B. Schöning-Burkhardt, A. Beyer, S. Müller, H. F. Abts, and K. Köhrer.** 2001. Mammalian cells express two VPS4 proteins both of which are involved in intracellular protein trafficking. J. Mol. Biol. **312:**469–480.
60. **Schneider, B. L., W. Seufert, B. Steiner, Q. H. Yang, and A. B. Futcher.** 1995. Use of polymerase chain reaction epitope tagging for protein tagging in *Saccharomyces cerevisiae*. Yeast **11:**1265–1274.
61. **Scott, A., J. Gaspar, M. D. Stuchell-Brereton, S. L. Alam, J. J. Skalicky, and W. I. Sundquist.** 2005. Structure and ESCRT-III protein interactions of the MIT domain of human VPS4A. Proc. Natl. Acad. Sci. USA **102:**13813–13818.
62. **Sorimachi, H., S. Ishiura, and K. Suzuki.** 1997. Structure and physiological function of calpains. Biochem. J. **328:**721–732.
63. **Sorimachi, H., and K. Suzuki.** 2001. The structure of calpain. J. Biochem. (Tokyo) **129:**653–664.
64. **Strack, B., A. Calistri, S. Craig, E. Popova, and H. G. Göttlinger.** 2003. AIP1/ALIX is a binding partner for HIV-1 p6 and EIAV p9 functioning in virus budding. Cell **114:**689–699.
65. **Strobl, S., C. Fernandez-Catalan, M. Braun, R. Huber, H. Masumoto, K. Nakagawa, A. Irie, H. Sorimachi, G. Bourenkow, H. Bartunik, K. Suzuki, and W. Bode.** 2000. The crystal structure of calcium-free human m-calpain suggests an electrostatic switch mechanism for activation by calcium. Proc. Natl. Acad. Sci. USA **97:**588–592.
66. **Suzuki, K., S. Hata, Y. Kawabata, and H. Sorimachi.** 2004. Structure, activation, and biology of calpain. Diabetes **53**(Suppl. 1)**:**S12–S18.
67. **Tian, L., R. A. Holmgren, and A. Matouschek.** 2005. A conserved processing mechanism regulates the activity of transcription factors Cubitus interruptus and NF-κB. Nat. Struct. Mol. Biol. **12:**1045–1053.
68. **Tilburn, J., J. C. Sánchez-Ferrero, E. Reoyo, H. N. Arst, Jr., and M. Á. Peñalva.** 2005. Mutational analysis of the pH signal transduction component PalC of *Aspergillus nidulans* supports distant similarity to BRO1 domain family members. Genetics **171:**393–401.
69. **Tilburn, J., S. Sarkar, D. A. Widdick, E. A. Espeso, M. Orejas, J. Mungroo, M. Á. Peñalva, and H. N. Arst, Jr.** 1995. The *Aspergillus* PacC zinc finger transcription factor mediates regulation of both acid- and alkaline-expressed genes by ambient pH. EMBO J. **14:**779–790.
70. **Tompa, P., P. Buzder-Lantos, A. Tantos, A. Farkas, A. Szilágyi, Z. Bánóczi, F. Hudecz, and P. Friedrich.** 2004. On the sequential determinants of calpain cleavage. J. Biol. Chem. **279:**20775–20785.
71. **Tsang, H. T., J. W. Connell, S. E. Brown, A. Thompson, E. Reid, and C. M. Sanderson.** 2006. A systematic analysis of human CHMP protein interactions: additional MIT domain-containing proteins bind to multiple components of the human ESCRT III complex. Genomics **88:**333–346.
72. **Urban, S., and M. Freeman.** 2002. Intramembrane proteolysis controls diverse signalling pathways throughout evolution. Curr. Opin. Genet. Dev. **12:**512–518.
73. **Vincent, O., L. Rainbow, J. Tilburn, H. N. Arst, Jr., and M. Á. Peñalva.** 2003. YPXL/I is a protein interaction motif recognized by *Aspergillus* PalA and its human homologue, AIP1/Alix. Mol. Cell. Biol. **23:**1647–1655.
74. **Vogel, J. L., and T. M. Kristie.** 2006. Site-specific proteolysis of the transcriptional coactivator HCF-1 can regulate its interaction with protein cofactors. Proc. Natl. Acad. Sci. USA **103:**6817–6822.
75. **von Schwedler, U. K., M. Stuchell, B. Müller, D. M. Ward, H. Y. Chung, E. Morita, H. E. Wang, T. Davis, G. P. He, D. M. Cimbora, A. Scott, H. G. Kräusslich, J. Kaplan, S. G. Morham, and W. I. Sundquist.** 2003. The protein network of HIV budding. Cell **114:**701–713.
76. **Wolfe, M. S., and R. Kopan.** 2004. Intramembrane proteolysis: theme and variations. Science **305:**1119–1123.
77. **Wootton, J. C., and S. Federhen.** 1996. Analysis of compositionally biased regions in sequence databases. Methods Enzymol. **266:**554–571.
78. **Xu, W., and A. P. Mitchell.** 2001. Yeast PalA/AIP1/Alix homolog Rim20p associates with a PEST-like region and is required for its proteolytic cleavage. J. Bacteriol. **183:**6917–6923.
79. **Xu, W., F. J. Smith, Jr., R. Subaran, and A. P. Mitchell.** 2004. Multivesicular body-ESCRT components function in pH response regulation in *Saccharomyces cerevisiae* and *Candida albicans*. Mol. Biol. Cell **15:**5528–5537.